Higher order Galerkin time discretization for nonstationary incompressible flow

S. Hussain, F. Schieweck, S. Turek

Abstract In this paper, we extend our work for the heat equation in [4] and for the Stokes equations in [5] to the nonstationary Navier-Stokes equations in two dimensions. We examine *continuous* Galerkin-Petrov (cGP) time discretization schemes for nonstationary incompressible flow. In particular, we implement and analyze numerically the higher order cGP(2)-method. For the space discretization, we use the LBB-stable finite element pair Q_2/P_1^{disc}. The discretized systems of nonlinear equations are treated by using the fixed-point as well as the Newton method and the associated linear subproblems are solved by using a monolithic multigrid solver with GMRES method as smoother. We perform nonstationary simulations for a benchmarking configuration to analyze the temporal accuracy and efficiency of the presented time discretization scheme.

Keywords: Continuous Galerkin-Petrov method, Navier-Stokes equations, multigrid method, Vanka smoother

2000 Mathematics Subject Classification (MSC): 65M12, 65M55, 65M60

1 Introduction

A class of time discretization schemes which is based on Rothe's method is the *continuous* Galerkin-Petrov discretization (cGP(k)-methods) and *discontinuous* Galerkin

Shafqat Hussain
Institut für Angewandte Mathematik, TU-Dortmund, Vogelpothsweg 87, 44227 Dortmund, Germany, e-mail: shafqat.hussain@math.tu-dortmund.de

Friedhelm Schieweck
Institut für Analysis und Numerik, Otto-von-Guericke-Universität Magdeburg, Postfach 4120, D-39016 Magdeburg, Germany, e-mail: schiewec@ovgu.de

Stefan Turek
Institut für Angewandte Mathematik, TU-Dortmund, Vogelpothsweg 87, 44227 Dortmund, Germany, e-mail: stefan.turek@math.tu-dortmund.de

(dG(k)-methods). The approach of the cGP-method has already been used by Aziz and Monk [1] (but not under this name) for the linear heat equation. These time discretizations are found to be of higher order and have been studied for the heat equation in [4] and for the Stokes equations in [5].

In this paper, we want to extend this numerical study for the nonstationary Navier-Stokes equations. In particular, we implement and analyze numerically the cGP(2)-method which is found to be of higher order at comparable numerical cost. The cGP(2)-method is of order 3 in the whole time interval and superconvergent of order 4 in the discrete time points. The spatial discretization is carried out by using biquadratic finite elements for the velocity and discontinuous linear elements for pressure. ¿From the numerical studies [4, 5], we have observed that the estimated experimental orders of convergence confirm the expected theoretical orders. Furthermore, the tests have shown that the cGP(2)-scheme provides significantly more accurate numerical solutions for both velocity and pressure than the other presented schemes cGP(1) and dG(1)-method (see [4, 5] for comparison).

Since we obtain superconvergence results for the velocity only at the discrete time points t_n, it is also desirable to get a high order pressure at the same points, for instance, for the computation of the hydrodynamic forces in CFD problems such as drag, lift etc. In order to get a higher order pressure, we perform a special post processing as described in [5].

The resulting discretized system of nonlinear equations which is characterized as a saddle point problem is treated by using the fixed-point and Newton method. The associated linear subproblems are solved by using a coupled multigrid solver with a local pressure Schur complement type smoother. Finally, we perform simulations for nonstationary flow problems to demonstrate the high accuracy of the cGP(2)-method. The test problem which is considered in this paper corresponds to the classical 'flow around cylinder' benchmark [8].

2 Galerkin time stepping for the Navier-Stokes equations

We consider the nonstationary incompressible Navier-Stokes equations, i.e. we want to find a velocity $\mathbf{u}$ and a pressure p *such that*

$$\begin{aligned} \partial_t \mathbf{u} - \nu \triangle \mathbf{u} + (\mathbf{u}\cdot\nabla)\mathbf{u} + \nabla p &= f, && \text{in} \quad \Omega \times (0,T), \\ \operatorname{div} \mathbf{u} &= 0 && \text{in} \quad \Omega \times (0,T), \\ \mathbf{u} &= 0 && \text{on} \quad \partial\Omega \times [0,T], \\ \mathbf{u}(x,0) &= \mathbf{u}_0(x) && \text{in} \quad \Omega \quad \text{for} \quad t = 0, \end{aligned} \tag{1}$$

where ν denotes the viscosity, f is the body force and $\mathbf{u}_0$ the initial velocity field at time $t = 0$. For simplicity, we restrict to 2D and we assume homogeneous Dirichlet conditions at the boundary $\partial\Omega$ of a polygonal domain Ω (for other choices see [3]). To make this problem well-posed in the case of pure Dirichlet boundary conditions, we have to look for p in the subspace $L^2_0(\Omega) \subset L^2(\Omega)$ of func-

tions with zero integral mean value. For the time discretization, we decompose the time interval $I = [0,T]$ into N subintervals $I_n := (t_{n-1}, t_n]$, where $n = 1,\dots,N$ and $0 = t_0 < t_1 < \cdots < t_{N-1} < t_N = T$. The symbol τ denotes the *time discretization parameter* and is also used as the maximum time step size $\tau := \max_{1\le n\le N} \tau_n$, where $\tau_n := t_n - t_{n-1}$. Then, for the subsequent continuous and discontinuous Galerkin time stepping schemes, we approximate the solution $\mathbf{u}$ by means of a function $\mathbf{u}_\tau$ which is piecewise polynomial of order k with respect to time, i.e., we are looking for $\mathbf{u}_\tau$ in the discrete time space (with $\mathbf{V} = (H_0^1(\Omega))^2$)

$$\mathbf{X}_\tau^k := \{\mathbf{u} \in C(I,\mathbf{V}) : \mathbf{u}\big|_{I_n} \in \mathbb{P}_k(I_n,\mathbf{V}) \quad \forall\, n = 1,\dots,N\}, \tag{2}$$

where

$$\mathbb{P}_k(I_n,\mathbf{V}) := \Big\{\mathbf{u} : I_n \to \mathbf{V} : \mathbf{u}(t) = \sum_{j=0}^{k} \mathbf{U}^j t^j\,,\ \forall t \in I_n,\ \mathbf{U}^j \in \mathbf{V},\ \forall\, j\Big\}.$$

Moreover, we introduce the discrete time test space

$$\mathbf{Y}_\tau^{k-1} := \{\mathbf{v} \in L^2(I,\mathbf{V}) : \mathbf{v}\big|_{I_n} \in \mathbb{P}_{k-1}(I_n,\mathbf{V}) \quad \forall\, n = 1,\dots,N\} \tag{3}$$

consisting of piecewise polynomials of order $k-1$ which are (globally) discontinuous at the end points of the time intervals. Similarly, we will use for the time-discrete pressure p_τ an analogous ansatz space $\tilde{X}_\tau^k$, where the vector valued space $\mathbf{V}$ is replaced by the scalar valued space $Q = L_0^2(\Omega)$, and an analogous discontinuous test space $\tilde{Y}_\tau^{k-1}$.

Now, in order to derive the time discretization, we multiply the equations in (1) with some suitable I_n-supported test functions and integrate over $\Omega \times I_n$. To determine $\mathbf{u}_\tau|_{I_n}$ and $p_\tau|_{I_n}$ we represent them by the polynomial ansatz

$$\mathbf{u}_\tau|_{I_n}(t) := \sum_{j=0}^{k} \mathbf{U}_n^j \phi_{n,j}(t), \qquad p_\tau|_{I_n}(t) := \sum_{j=0}^{k} P_n^j \phi_{n,j}(t), \tag{4}$$

where the "coefficients" $(\mathbf{U}_n^j, P_n^j)$ are elements of the function spaces $\mathbf{V} \times Q$ and the polynomial functions $\phi_{n,j} \in \mathbb{P}_k(I_n)$ are the Lagrange basis functions with respect to the $k+1$ nodal points $t_{n,j} \in I_n$ satisfying the conditions

$$\phi_{n,j}(t_{n,i}) = \delta_{i,j}, \qquad i,j = 0,\dots,k \tag{5}$$

with the Kronecker symbol $\delta_{i,j}$. For an easy treatment of the initial condition, we set $t_{n,0} = t_{n-1}$. Then, the initial condition is equivalent to the condition

$$\mathbf{U}_n^0 = \mathbf{u}_\tau|_{I_{n-1}}(t_{n-1}) \quad \text{if} \quad n \ge 2 \qquad \text{or} \qquad \mathbf{U}_n^0 = \mathbf{u}_0 \quad \text{if} \quad n = 1. \tag{6}$$

The other points $t_{n,1},\dots,t_{n,k}$ are chosen as the quadrature points of the k-point Gaussian formula on I_n which is exact if the function to be integrated is a polynomial of degree less or equal to $2k-1$. We define the basis functions $\phi_{n,j} \in \mathbb{P}_k(I_n)$ of (4) via

affine reference transformations (see [4, 5] for more details). Now, we can describe the *time discrete I_n-problem of the cGP(k)-method* [4, 6]:

Find on the interval $I_n = (t_{n-1}, t_n]$ the k unknown pairs of "coefficients" $(\mathbf{U}_n^j, P_n^j) \in \mathbf{V} \times Q$, $j = 1, \ldots, k$, such that for all $i = 1, \ldots, k$, it holds for all $\mathbf{v} \in \mathbf{V},\ q \in Q$

$$\begin{aligned} \sum_{j=0}^{k} \alpha_{i,j} \left(\mathbf{U}_n^j, \mathbf{v}\right)_\Omega + \frac{\tau_n}{2} a(\mathbf{U}_n^i, \mathbf{v}) + \frac{\tau_n}{2} n(\mathbf{U}_n^i, \mathbf{U}_n^i, \mathbf{v}) + \frac{\tau_n}{2} b(\mathbf{v}, P_n^i) &= \tfrac{\tau_n}{2} \left(f(t_{n,i}), \mathbf{v}\right)_\Omega, \\ b(\mathbf{U}_n^i, q) &= 0, \end{aligned} \tag{7}$$

with $\mathbf{U}_n^0 := \mathbf{u}_\tau(t_{n-1})$ for $n > 1$ and $\mathbf{U}_1^0 := \mathbf{u}_0$. Here, $\alpha_{i,j}$ denote some constants independent of τ_n and $(\cdot,\cdot)_\Omega$ the usual inner product in $L^2(\Omega)$. The bilinear form $a(\cdot,\cdot)$ on $\mathbf{V} \times \mathbf{V}$, $b(\cdot,\cdot)$ on $\mathbf{V} \times Q$ and the trilinear form $n(\cdot,\cdot,\cdot)$ on $\mathbf{V} \times \mathbf{V} \times \mathbf{V}$, respectively, are defined by

$$a(\mathbf{u}, \mathbf{v}) := \int_\Omega \nabla \mathbf{u} \cdot \nabla \mathbf{v}\, dx,\ \ b(\mathbf{v}, p) := -\int_\Omega \nabla \cdot \mathbf{v}\, p\, dx,\ \ n(\mathbf{w}, \mathbf{u}, \mathbf{v}) := \int_\Omega (\mathbf{w} \cdot \nabla)\mathbf{u} \cdot \mathbf{v}\, dx.$$

In the following, we specify the cGP(k)-method for the case $k = 2$ where the discretization error in the L^2-norm is superconvergent of order 4 at the discrete time points.

2.1 The cGP(2)-method

Here, we use the 2-point Gaussian formula with the quadrature points $\hat{t}_1 = -\frac{1}{\sqrt{3}}$ and $\hat{t}_2 = \frac{1}{\sqrt{3}}$ at the reference interval $(-1, 1]$. Then, the coefficients in (7) are

$$(\alpha_{i,j}) = \begin{pmatrix} -\sqrt{3} & \frac{3}{2} & \frac{2\sqrt{3}-3}{2} \\ \sqrt{3} & \frac{-2\sqrt{3}-3}{2} & \frac{3}{2} \end{pmatrix} \qquad i = 1, 2,\ j = 0, 1, 2.$$

Consequently, on the time interval I_n, we have to solve for the two "unknowns"

$$(\mathbf{U}_n^j, P_n^j) = \left(\mathbf{u}_\tau(t_{n,j}), p_\tau(t_{n,j})\right) \in \mathbf{V} \times Q \qquad \text{with} \qquad t_{n,j} := T_n(\hat{t}_j) \quad \text{for} \quad j = 1, 2,$$

where $T_n : (-1, 1] \to I_n$ denotes the affine reference mapping. The corresponding coupled system reads

$$\begin{aligned} \alpha_{1,1} \left(\mathbf{U}_n^1, \mathbf{v}\right)_\Omega + \tfrac{\tau_n}{2} a(\mathbf{U}_n^1, \mathbf{v}) + \tfrac{\tau_n}{2} n(\mathbf{U}_n^1, \mathbf{U}_n^1, \mathbf{v}) + \alpha_{1,2} \left(\mathbf{U}_n^2, \mathbf{v}\right)_\Omega + \tfrac{\tau_n}{2} b(\mathbf{v}, P_n^1) &= \ell_1(\mathbf{v}) \\ \alpha_{2,1} \left(\mathbf{U}_n^1, \mathbf{v}\right)_\Omega + \alpha_{2,2} \left(\mathbf{U}_n^2, \mathbf{v}\right)_\Omega + \tfrac{\tau_n}{2} a(\mathbf{U}_n^2, \mathbf{v}) + \tfrac{\tau_n}{2} n(\mathbf{U}_n^2, \mathbf{U}_n^2, \mathbf{v}) + \tfrac{\tau_n}{2} b(\mathbf{v}, P_n^2) &= \ell_2(\mathbf{v}) \\ b(\mathbf{U}_n^1, q) &= 0 \\ b(\mathbf{U}_n^2, q) &= 0, \end{aligned} \tag{8}$$

which has to be satisfied for all $\mathbf{v} \in \mathbf{V}$ and $q \in Q$ with the linear functionals

$$\ell_i(\mathbf{v}) := \frac{\tau_n}{2}\left(f(t_{n,i}),\mathbf{v}\right)_\Omega - \alpha_{i,0}\left(\mathbf{U}_n^0,\mathbf{v}\right)_\Omega \qquad i=1,2. \tag{9}$$

Once we have determined the solutions $(\mathbf{U}_n^j, P_n^j)$ at the Gaussian points in the interior of the interval I_n, we get the solution at the right boundary t_n of I_n by means of quadratic extrapolation from the ansatz (4), i.e.,

$$\mathbf{u}_\tau(t_n) = \mathbf{U}_n^0 + \sqrt{3}(\mathbf{U}_n^2 - \mathbf{U}_n^1), \tag{10}$$

where $\mathbf{U}_n^0$ is the initial value at the time interval I_n.

After discretizing equation (1) in time, we now discretize the resulting "I_n-problems" (8) in space by using the finite element method [7, 2] with the well-known Q_2/P_1^{disc} element. Here, we present only the resulting block system for the nodal vectors $\underline{\mathbf{U}}_n^j = (\underline{U}_n^j, \underline{V}_n^j)$ and $\underline{P}_n^j$, $j=1,2$, associated with the finite element functions that approximate the functions $\mathbf{U}_n^j \in \mathbf{V}$ and $P_n^j \in Q$ in (8). The 6×6 block system on the time interval I_n reads:

For given initial velocity $\underline{\mathbf{U}}_n^0 = (\underline{U}_n^0, \underline{V}_n^0)$, find the nodal vectors $\underline{\mathbf{U}}_n^j = (\underline{U}_n^j, \underline{V}_n^j)$ and $\underline{P}_n^j$, $j=1,2$, such that for

$$u = (\underline{U}_n^1, \underline{U}_n^2), \quad v = (\underline{V}_n^1, \underline{V}_n^2), \quad p = (\tau_n \underline{P}_n^1, \tau_n \underline{P}_n^2),$$

it holds

$$\begin{bmatrix} A(u,v) & 0 & B_u \\ 0 & A(u,v) & B_v \\ B_u^T & B_v^T & 0 \end{bmatrix} \begin{bmatrix} u \\ v \\ p \end{bmatrix} = \begin{bmatrix} R_u \\ R_v \\ 0 \end{bmatrix} \tag{11}$$

where

$$A(u,v) = \begin{bmatrix} 3M + \tau_n L + \tau_n N_1(u,v) & \left(2\sqrt{3}-3\right)M \\ \left(-2\sqrt{3}-3\right)M & 3M + \tau_n L + \tau_n N_2(u,v) \end{bmatrix},$$

$$B_u = \begin{bmatrix} B_1 & 0 \\ 0 & B_1 \end{bmatrix}, \qquad B_v = \begin{bmatrix} B_2 & 0 \\ 0 & B_2 \end{bmatrix}$$

and $N_1(u,v) = N(\underline{U}_n^1, \underline{V}_n^1)$, $N_2(u,v) = N(\underline{U}_n^2, \underline{V}_n^2)$ correspond to the nonlinear operators evaluated at the Gauß points $t_{n,1}$ and $t_{n,2}$, respectively.

Here, M, L, B_1, B_2 denote the mass, Laplacian and pressure matrices, respectively. The right hand side vectors $R_u = (R_u^1, R_u^2)$ and $R_v = (R_v^1, R_v^2)$ are given by

$$R_u^j := \tau_n F_n^j - 2\sqrt{3}(-1)^j M \underline{U}_n^0, \qquad R_v^j := \tau_n G_n^j - 2\sqrt{3}(-1)^j M \underline{V}_n^0, \qquad j=1,2,$$

where F_n^j and G_n^j are the vectors corresponding to the term $\left(f(t_{n,j}),\mathbf{v}\right)_\Omega$ with test functions $\mathbf{v} = (\varphi_i, 0)$ and $\mathbf{v} = (0, \varphi_i)$, respectively ($\varphi_i$ denoting the scalar basis functions for velocity).

Once we have determined the solutions $\underline{\mathbf{U}}_n^j = (\underline{U}_n^j, \underline{V}_n^j)$, $j=1,2$, we compute the nodal vector $\underline{\mathbf{U}}_{n+1}^0 = (\underline{U}_{n+1}^0, \underline{V}_{n+1}^0)$ of the fully discrete solution $\mathbf{u}_{\tau,h}(t_n) = (u_{\tau,h}(t_n), v_{\tau,h}(t_n))$ at time t_n by using the following quadratic extrapolation

$$u_{\tau,h}(t_n) \sim \underline{U}_{n+1}^0 := \underline{U}_n^0 + \sqrt{3}(\underline{U}_n^2 - \underline{U}_n^1), \qquad v_{\tau,h}(t_n) \sim \underline{V}_{n+1}^0 := \underline{V}_n^0 + \sqrt{3}(\underline{V}_n^2 - \underline{V}_n^1).$$

3 Numerical Results

In this section, we perform nonstationary simulations to demonstrate the temporal accuracy and efficiency of the presented time discretization scheme. As a test problem, we consider the *flow around cylinder* which exactly corresponds to the benchmark configuration in [8]. In this simulation, we concentrate only on the nonstationary behavior of the flow pattern with periodic oscillations and examine the ability of the presented time discretization scheme to capture the dynamics of the flow. Details regarding the benchmark settings can be found at `www.featflow.de/en/benchmarks/cfdbenchmarking.html`. The examined accuracy of the benchmark crucially depends on the following quantities

$$F_D = \int_S (\rho \nu \frac{\partial u_t}{\partial n} n_y - p n_x) dS, \quad \text{and particularly} \quad F_L = -\int_S (\rho \nu \frac{\partial u_t}{\partial n} n_x - p n_y) dS$$

representing the total forces in the horizontal and vertical directions, respectively. Figure 1 shows the initial coarse mesh (level 1), which will be uniformly refined,

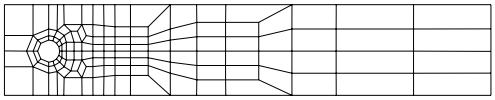

Lev.	#EL	#DOF(total)
2	520	5 928
3	2 080	23 296
4	8 320	92 352

Fig. 1 Coarse mesh for the *flow around cylinder*. **Fig. 2** Size of the different systems in space.

and Figure 2 presents for different space mesh levels the number '#EL' of elements and the total number '#DOF' of degrees of freedom. In order to demonstrate the accuracy of the higher order time discretization, the flow is started from the same developed solution at time t_0, and the simulation is performed until T=10 for various uniform time step sizes $\tau_n := \tau$. After T=10, all the introduced quantities are plotted and analyzed in detail. Here, we will concentrate on the values of the lift coefficient (C_L). To this end, we show in Figure 3 only the zoomed picture in the last time unit from T=9 to T=10 at space level 4.

Next, we present a more quantitative analysis than on the basis of plots in Figure 3. For different time step sizes τ, Table 1 shows the 'deviation in percentage of the curves per cycle' from a reference curve. We can see that the maximum time step

τ	**Lev=2**	**Lev=3**	**Lev=4**
1/100	0.00%	0.00%	0.00%
1/50	0.01%	0.01%	0.01%
1/25	0.11%	0.13%	0.12%
1/20	0.25%	0.29%	0.29%
1/15	0.72%	0.84%	0.85%
1/10	0.93%	0.96%	0.98%

Table 1 Changes of the lift values in percentage at given space level.

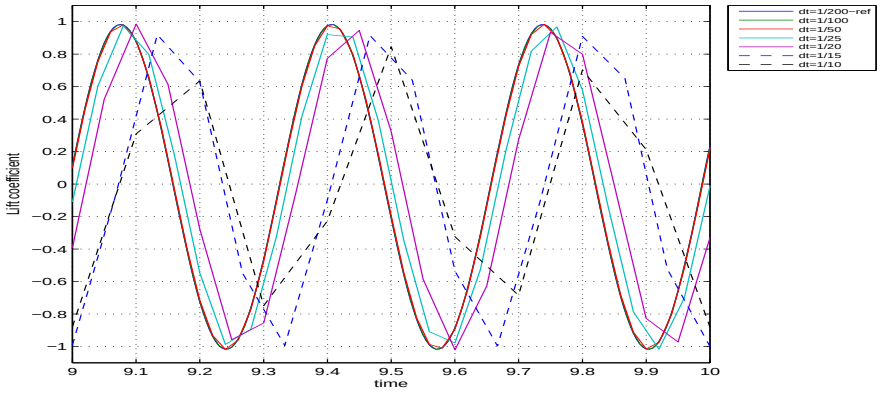

Fig. 3 Lift coefficient for different Δt using cGP(2)-method at space mesh level 4.

size to gain the accuracy with an error of less than 1% per period for the cGP(2)-method is $\tau = 1/10$.

4 Solver Analysis

In order to measure the efficiency of the nonlinear solver for the presented time discretization scheme, we show in Table 2 the averaged number '#NL' of nonlinear iterations per time step for the fixed-point (FP) and Newton (NWT) method on different space mesh levels. To analyze the corresponding behavior of the multigrid solver for the solution of linear subproblems, we present the averaged number '#MG' of multigrid iterations per (nonlinear) step. Here, the multigrid solver uses a preconditioned GMRES method (preconditioned with a cell oriented Vanka scheme) as smoother and applies four pre- and post-smoothing steps. Table 2 reveals that, for

τ	**FP**	**NWT**	**FP**	**NWT**	**FP**	**NWT**	**FP**	**NWT**	**FP**	**NWT**	**FP**	**NWT**
	#NL	#NL	#NL	#NL	#NL	#NL	#MG	#MG	#MG	#MG	#MG	#MG
	Level=3		Level=4		Level=5		Level=3		Level=4		Level=5	
1/10	11.18	5.00	10.18	4.91	9.00	4.55	10.91	10.60	10.20	9.60	9.11	9.00
1/15	8.62	4.06	7.94	4.00	7.00	4.00	10.89	10.20	10.50	10.00	9.43	9.25
1/20	7.14	4.00	7.00	4.00	6.00	3.90	11.00	10.75	10.71	10.25	9.67	9.25
1/25	7.00	4.00	6.00	3.04	5.04	3.04	11.43	11.00	11.00	10.25	9.50	9.25
1/50	5.02	3.02	4.24	3.00	4.02	3.00	11.83	11.00	11.60	10.67	10.00	9.67
1/100	4.01	2.01	3.98	2.01	3.01	2.01	11.60	11.00	12.00	11.33	11.00	10.33
1/200	3.00	2.00	3.00	2.00	3.00	2.00	12.00	11.00	12.50	12.00	12.00	11.33

Table 2 Averaged number of nonlinear iterations (#NL) per time step and multigrid linear iterations (#MG) per nonlinear step.

both nonlinear solver methods, almost the same number of iterations are required if τ is fixed and the space mesh level increases. Moreover, for fixed space mesh level, the number of nonlinear iterations decreases if the time step size is reduced, as expected. Concerning the number of nonlinear iterations, Table 2 shows that the Newton method is more efficient than the fixed point iteration. We also see that the number of multigrid iterations remains fairly constant if we increase the refinement level of the space mesh. There is also no noticeable increase in the number of iterations if we decrease the time step size. This means that the behavior of the multigrid solver is almost independent of the space mesh size and the time step size.

5 Conclusion

We have implemented the cGP(2)-method for the nonstationary Navier-Stokes equations. The spatial discretization is carried out by using biquadratic finite elements for velocity and discontinuous linear elements for pressure. The discretized systems of nonlinear equations are treated by means of the fixed-point and the Newton method. The associated linear systems have been solved using a geometrical multigrid method with the Vanka-type preconditioned GMRES method as smoother. ¿From the numerical studies, we observe that the cGP(2)-scheme provides highly accurate numerical solutions at quite large time step sizes. Moreover, the analysis of the numerical costs shows that the arising nonlinear block-systems in the implicit time discretization scheme can be solved very efficiently with nearly optimal complexity.

References

1. Aziz, A.K., Monk, P.: Continuous finite elements in space and time for the heat equation. Math. Comp. **52**(186), 255–274 (1989)
2. C. Cuvelier, A. Segal, A. A. Steenhoven: Finite element methods and Navier-Stokes equations. D. Reidel Publishing Company (1986)
3. Heywood, J., Rannacher, R., Turek, S.: Artificial boundaries and flux and pressure conditions for the incompressible Navier–Stokes equations. International Journal for Numerical Methods in Fluids **22**, 325–352 (1996)
4. Hussain, S., Schieweck, F., Turek, S.: Higher order Galerkin time discretizations and fast multigrid solvers for the heat equation. Journal of Numerical Mathematics **19**(1), 41–61 (2011)
5. Hussain, S., Schieweck, F., Turek, S.: A note on accurate and efficient higher order Galerkin time stepping schemes for the nonstationary Stokes equations. The Open Numerical Methods Journal (2011). Accepted for publication
6. Schieweck, F.: A-stable discontinuous Galerkin-Petrov time discretization of higher order. J. Numer. Math. **18**(1), 25 – 57 (2010)
7. Thomée, V.: Galerkin finite element methods for parabolic problems, *Springer Series in Computational Mathematics*, vol. 25, second edn. Springer-Verlag, Berlin (2006)
8. Turek, S., Schäfer, M.: Benchmark computations of laminar flow around cylinder. In: E. Hirschel (ed.) Flow Simulation with High-Performance Computers II, *Notes on Numerical Fluid Mechanics*, vol. 52, pp. 547–566. Vieweg (1996)